

Figure 7-5 Diagram of Wall-Diaaphragm Tension Tie Failure (from Rutherford and Chekene, 1990)

plane overturning, gradual degradation and softening of the pier, and excessive out-of-plane residual displacements (“walking”) of the pier, leading to instability.

The strength and displacement capacities of an element in rocking are based on FEMA 273, where the “d” drift value of  $0.4h_e/L$  was established. Currently available experimental results are insufficient to determine the relative influence of number of cycles, drift, and ductility on rocking degradation. In the field, it is often difficult to find evidence of rocking, because the cracks close at the completion of shaking. However, horizontal cracks at the top and bottom of piers have been observed, particularly as pointing mortar spalls.

### 7.2.5 Bed-Joint Sliding

In this type of behavior, sliding occurs on bed joints. Commonly observed both in the field and in experimental tests, there are two basic forms: sliding on a horizontal plane, and a stair-stepped diagonal crack where the head joints open and close to allow for movement on the bed joint. See Figure 7-10 for an

example of typical stair-stepped bed-joint sliding observed in the field. Pure bed-joint sliding is a ductile mode with significant hysteretic energy dissipation capability. If sliding continues in the absence of one of the less-ductile modes noted in the sections that follow, then gradual degradation of the cracking region occurs until instability is reached. Theoretically possible, but not widely reported, is the case of stair-stepped cracking in which sliding goes so far that an upper brick slides off a lower brick.

The strength and displacement capacities (in shear) for bed-joint sliding are based on FEMA 273, which uses a Mohr-Coulomb model originally developed as part of the ABK research. A Mohr-Coulomb model includes a bond and friction component. There are many uncertainties in this model, in relating the *in-situ* testing to the model, and in the *in-situ* testing itself. The FEMA 273 equation for shear capacity is:

$$V_{bjs} = v_{me} A_n = A_n [0.75(0.75v_{te} + P_{CE}/A_n)] / 1.5 \quad (7-1)$$



**Figure 7-6** Photo of Wall-Diaphragm Tension Tie Failure (from Rutherford and Chekene, 1990)

where:

- $v_{te}$  = the average test value from in-place testing
- $P_{CE}$  = the expected gravity compressive force
- $A_n$  = the area of net mortared/grouted section.

The model was calibrated with limited empirical tests using brick units, which resulted in the first 0.75 coefficient. Calibrations for other types of masonry such as ungrouted CMU or HCT have not been done. The model is most appropriate for estimating strength before cracking; after cracking the bond capacity will

be eroded, and the strength is likely to be based on only the friction portion of the equation. Significant strength degradation has been observed in experiments at drifts of 0.3-0.4% which are likely to correspond to complete erosion of bond capacity. See Sections 7.3 and FEMA 307 for the implications of strength degradation due to sliding.

The  $v_{te}$  value representing bond strength is derived from the average of the individual push test values,  $v_{to}$ , adjusted for dead load by the equation:

$$v_{to} = V_{test}/A_b - p_{D+L}, \quad (7-2)$$

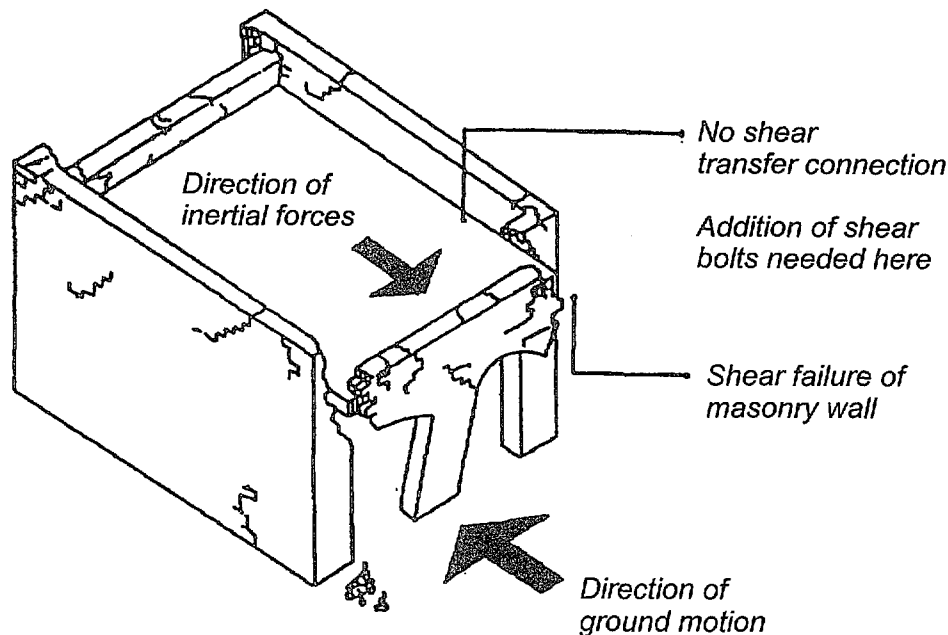


### Diagram of Shear Failure

A brick building can collapse in an earthquake if it lacks shear transfer connections

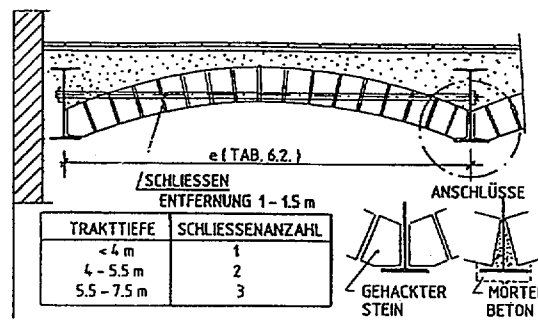
Figure 7-7 Diagram of Wall-Diaphragm Shear Tie Failure (from City of Los Angeles, 1991)

where:

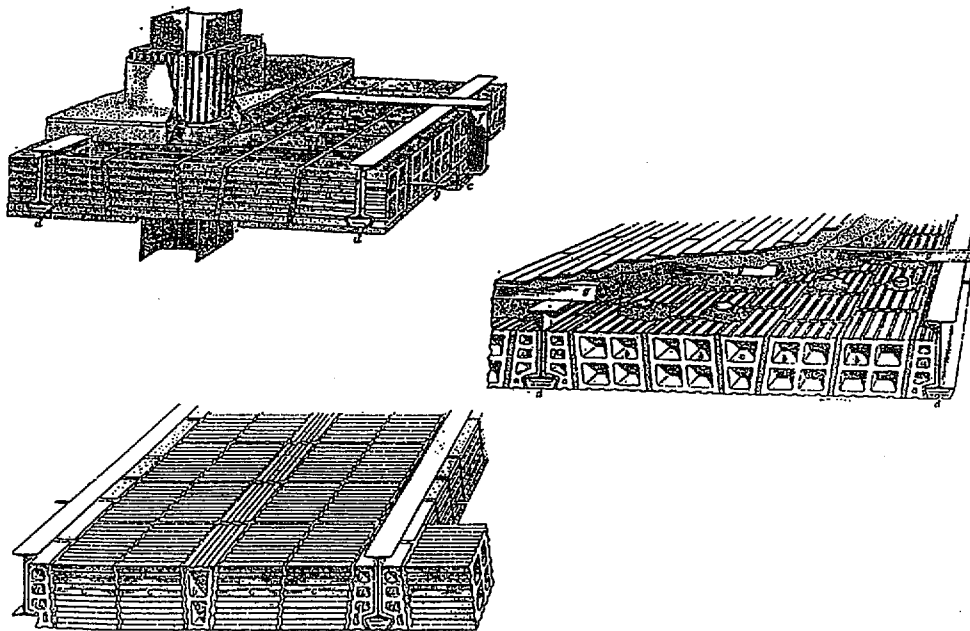
- $V_{test}$  = the test value  
 $A_b$  = the net mortared area of the bed joints above and below the test  
 $p_{D+L}$  = the estimated gravity stress at the test location.

$A_b$  does not include the potential resistance of the collar joint; the influence of collar-joint fill is applied later to the  $v_{me}$  equation with the second 0.75 factor. This factor is waived if collar-joint fill is not present. While this

simplifies the data reduction, it is less accurate than addressing the effect of fill in the collar joint at the test location itself. In many instances, it is difficult to determine the extent of the collar-joint fill. It can also be difficult to determine the actual gravity stress at a test location in walls with irregular openings. In some cases, flat-jack testing can be used to estimate gravity stresses. In FEMA 273, a 100 psi limit is set on  $v_{te}$ ; although such a limit may be appropriate for design purposes, it is inappropriate for evaluating actual damage. The 1.5 factor in the  $v_{te}$  equation is to relate the average shear of  $V/A_n$  to the critical shear value of  $1.5 V/A_n$ , as derived from a parabolic distribution of shear



(a) Brick arch spanning between steel I-beams



(b) Hollow clay tile flat arch spanning between steel I-beams

Figure 7-8 Examples of Various Masonry Diaphragms (from Rutherford and Chekene, 1997)

in a rectangular section. ABK (1984) indicates that the 1.5 factor may overestimate the critical shear in long walls without openings.

Finally, the in-place push test has a number of uncertainties. Experience has shown that test results can vary substantially within the same masonry class, with coefficients of variation of 0.30 or more when the required number of tests are performed. This may be due to actual material variations, but it is also probably due in part to the uncertainty in determining when “either a crack can be seen or slip occurs”—the

governing criteria in *UBC Standard 21-6* (ICBO, 1994) for determining the test load,  $V_{test}$ . Alternatives have been proposed to define  $V_{test}$  as the load occurring when the load-deflection curve stiffness is reduced to a certain percentage of the initial stiffness, or more simply, when a certain threshold deflection is reached.

### 7.2.6 Bed-Joint Sliding at Wall Base

Observed in experiments, this mode is a variation of bed-joint sliding in which the sliding occurs on the

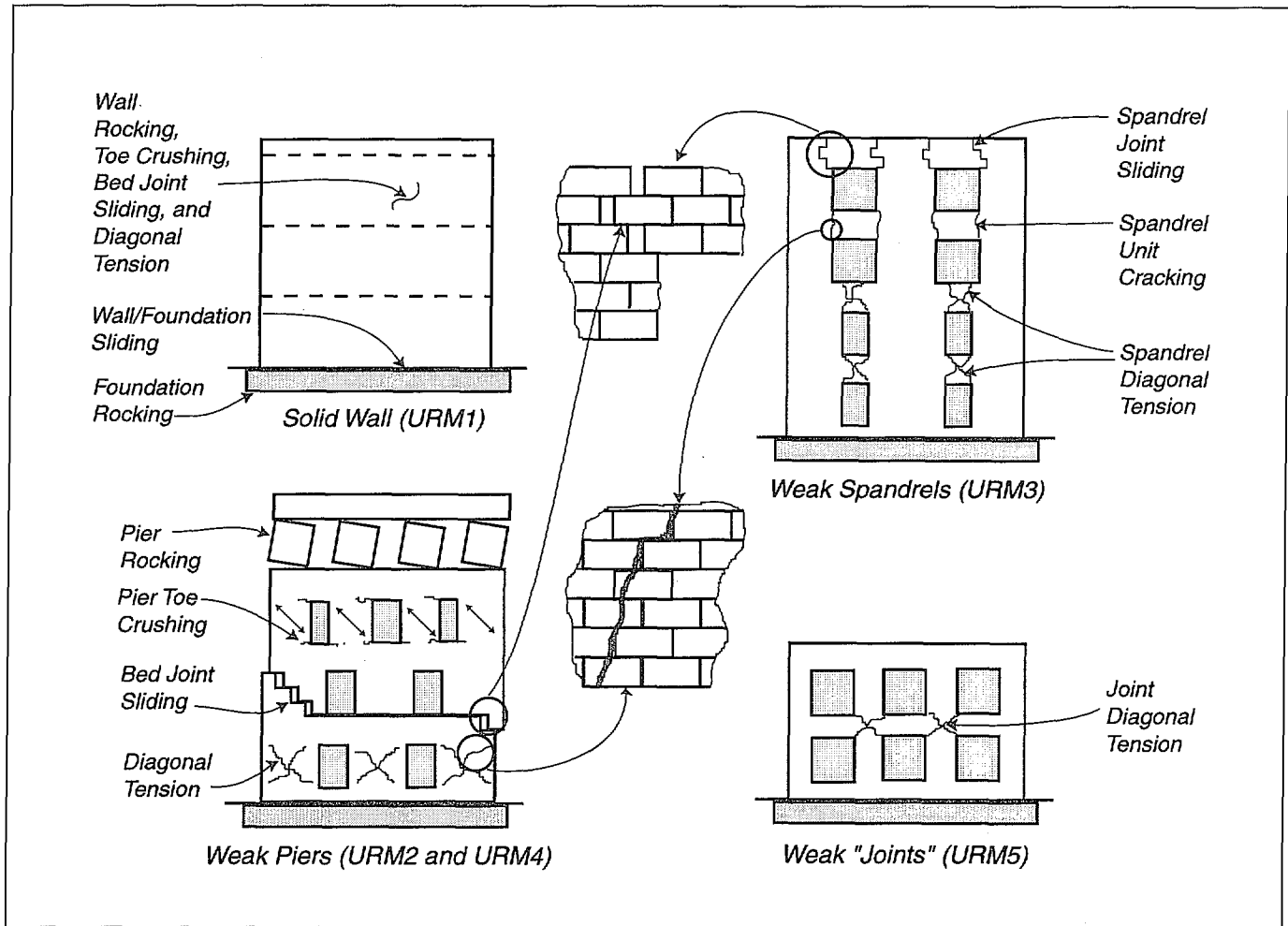


Figure 7-9 URM Wall Components

surface where the URM wall meets the foundation. Strength and displacement capacities are assumed to be similar to bed-joint sliding as described in Section 7.2.5.

### 7.2.7 Spandrel-Joint Sliding

Commonly observed in the field in running bond masonry, this form of bed-joint sliding in the ends of the spandrel resembles interlocked fingers pulling apart, and it occurs when the in-plane moment capacity of the spandrel is reached, but before the shear capacity of the spandrel is reached. This mode can be relatively ductile and can allow for significant drift, provided a reliable lintel is present. As the spandrel displaces, the nonlinear mechanism of response may move to other portions of the wall such as the piers.

The strength and displacement capacity are based on a modified version of the bed-joint sliding equation in FEMA 273. See Section 7.3 for details.

### 7.2.8 Rocking/Toe Crushing

This sequence of damage occurs when rocking (see Section 7.2.4) continues for several cycles, followed by an abrupt loss of capacity occurs as the toe crushes. Specimen W3 of Abrams and Shah (1992) is an example of such a phenomenon.

There is insufficient testing to determine parameters that would allow for an analytical determination of when rocking will degenerate into toe crushing. Intuitively, piers with higher axial stress and those subjected to higher drift levels and repeated cycles would be more likely to experience toe crushing. Because of the lack of data, this behavior is combined

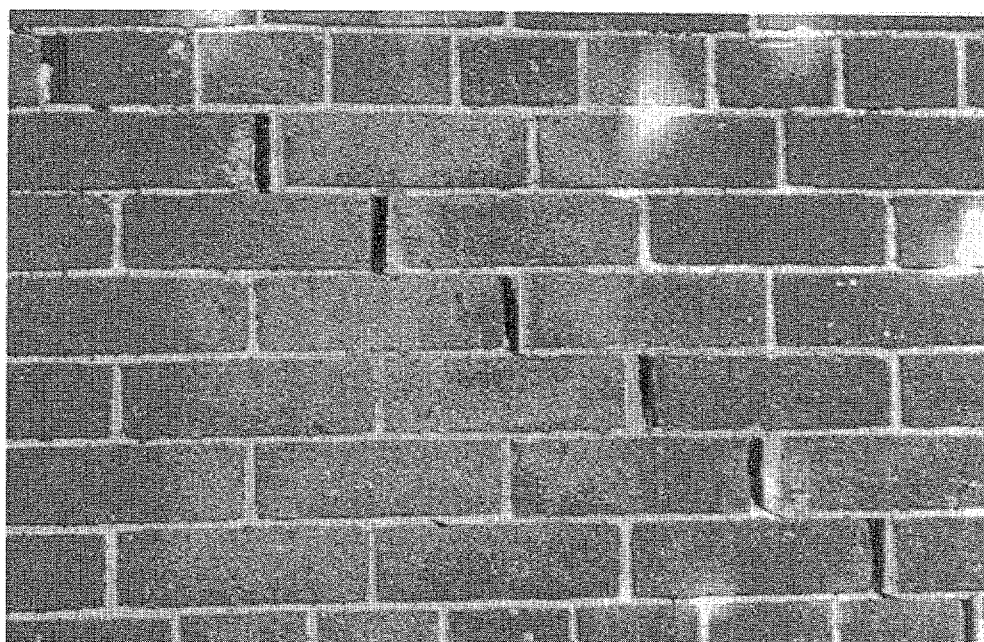


**Figure 7-10**      *Photo of Bed Joint Sliding*

in this document with typical rocking behavior, and rocking capacity is set conservatively in FEMA 273.

### **7.2.9 Flexural Cracking/Toe Crushing/Bed Joint Sliding**

In this sequence of behavior, flexural cracking occurs at the heel, but rocking does not begin. Instead, shear is redistributed to the toe, seismic forces increase, and a compression failure occurs in the toe. Diagonal cracks form, oriented toward the corners. Initial toe crushing is followed immediately by the ultimate limit state of bed-joint sliding.

This sequence was observed in Specimens W1, W2, and W3 of Manzouri et al. (1995). Initial capacity appears to be close to the FEMA 273 equation for toe crushing with a final capacity close to the frictional strength of the mortar. Under repeated cyclic loading, the toes may eventually deteriorate to the point of vertical instability. See FEMA 307 for commentary on this mode.

### **7.2.10 Flexural Cracking/Diagonal Tension**

In this mode of behavior, flexural racking occurs at the heel, but not rocking. Shear is redistributed to the toe, seismic forces increase, a diagonal tension crack

develops, and capacity can be rapidly lost. Cracking typically occurs in the units as well as the joints. See Section 7.2.14 for more details.

Strength capacity is assumed to be the same as the FEMA 273 equation for diagonal tension capacity; displacements of approximately 0.5% have been observed in tests.

### **7.2.11 Flexural Cracking/Toe Crushing**

In this sequence of behavior, flexural cracking occurs at the heel, but not rocking. Shear is redistributed to the toe, the seismic load increases, and a compression failure occurs in the toe. This type of behavior typically occurs in stockier walls with  $L/h_{eff} > 1.25$ . Based on laboratory testing of cantilever specimens, four steps can usually be identified. First, flexural cracking happens at the base of the wall, but it does not propagate all the way across the wall. This can also cause a series of horizontal cracks to form above the heel. Second, sliding occurs on bed joints in the central portion of the pier. Third, diagonal cracks form at the toe of the wall. Finally, large cracks form at the upper corners of the wall. Failure occurs when the triangular portion of wall above the crack rotates off the crack or

the toe crushes so significantly that vertical load carrying capability is compromised.

Testing is limited to five monotonic specimens in Epperson and Abrams (1989), which all exhibited similar behavior, and Specimen W2 in Abrams and Shah (1992), which was tested with quasistatic reversed-cyclic loading. The strength is well-predicted by the FEMA 273 toe crushing equation. Toe crushing is considered in FEMA 273 to be a force-controlled mode, but moderate ductility was observed in Epperson and Abrams (1989), with drift values at conclusion of the test equal to 0.2-0.4%. In the Abrams and Shah (1992) test, even higher drift appears to have been achieved. Thus, some moderate degree of nonlinear capacity is possible. As noted above, behavior is similar to the Manzouri et al. (1995) tests, except that bed-joint sliding at the base did not occur at higher drifts.

### 7.2.12 Spandrel-Unit Cracking

In this type of damage, the moment at the end of the spandrel is not relieved by sliding, but instead causes brittle vertical cracking through the masonry units. Depending on the lintel construction, this can lead to a local falling hazard. It also can alter the height of the piers.

The cracked portion of the spandrel is assumed to lack both shear and tensile capacity. As a result, only the uncracked section is assumed to contribute to the strength and displacement capacity. See Section 7.3 for details.

### 7.2.13 Corner Damage

This form of damage is commonly observed at the intersection of the roof and walls subjected to in-plane and out-of-plane demands in moderate earthquakes. See Figures 7-11 and 7-12 for a diagram and photo of this damage type. Although not studied in experiments, it is likely to result from a combination of any of three possible causes:

- When a roof diaphragm without shear anchorage moves parallel to the walls subjected to in-plane demands, the walls subjected to out-of-plane demands may be punched outward. The tensile capacity of the wall (from the strength of the bed joints) is exceeded locally, and the wall corner falls.
- Damage may be exacerbated by cracking resulting from the horizontal spanning of the wall. In a

horizontal span, there is bending restraint at the ends of the wall due to the returns around the corner. If the resulting moment at the wall ends exceeds the capacity, a vertical crack occurs at the corner.

- For walls with openings near the corner, in-plane demands force moments into the joint between the outer pier at the top story and the adjacent spandrel. The moment places tensile demands on the head and bed joints at the pier/spandrel intersection, causing a diagonal crack to form.

Capacities are difficult to identify for the first two causes; the third is covered in a methodology developed in Section 7.3.

### 7.2.14 Preemptive Diagonal Tension

In this behavior mode, a diagonal tension crack forms without significant ductile response. Typical diagonal tension cracking—resulting from strong mortar, weak units, and high compressive stress—can be identified by diagonal cracks (“X” cracks) that propagate through the units. In many cases, the cracking is sudden and brittle, and vertical load capacity drops quickly. The cracks may then extend to the toe, and the triangles above and below the crack separate. In a few cases, the load drop may be more gradual with cracks increasing in size and extent with each cycle.

A second form of diagonal tension cracking exists with weak mortar, strong units, and low compressive stress, when the cracks propagate in a stair-stepped manner in head and bed joints. In Specimen MA of Calvi and Magenes (1994), this behavior was observed (Magenes, 1997).

Capacity is based on the FEMA 273 equation for diagonal tension. This equation requires calculation of masonry tensile strength, but there is no direct test for this value. As a substitute, the bed-joint mortar strength is used. This strength value only applies to the mortar, not the masonry units. Thus, there is a great deal of uncertainty in diagonal tension-strength calculations.

### 7.2.15 Preemptive Toe Crushing

In this form of damage, compression at the toe causes crushing without significant ductile response, such as rocking. There are no reported experimental observations of such behavior.

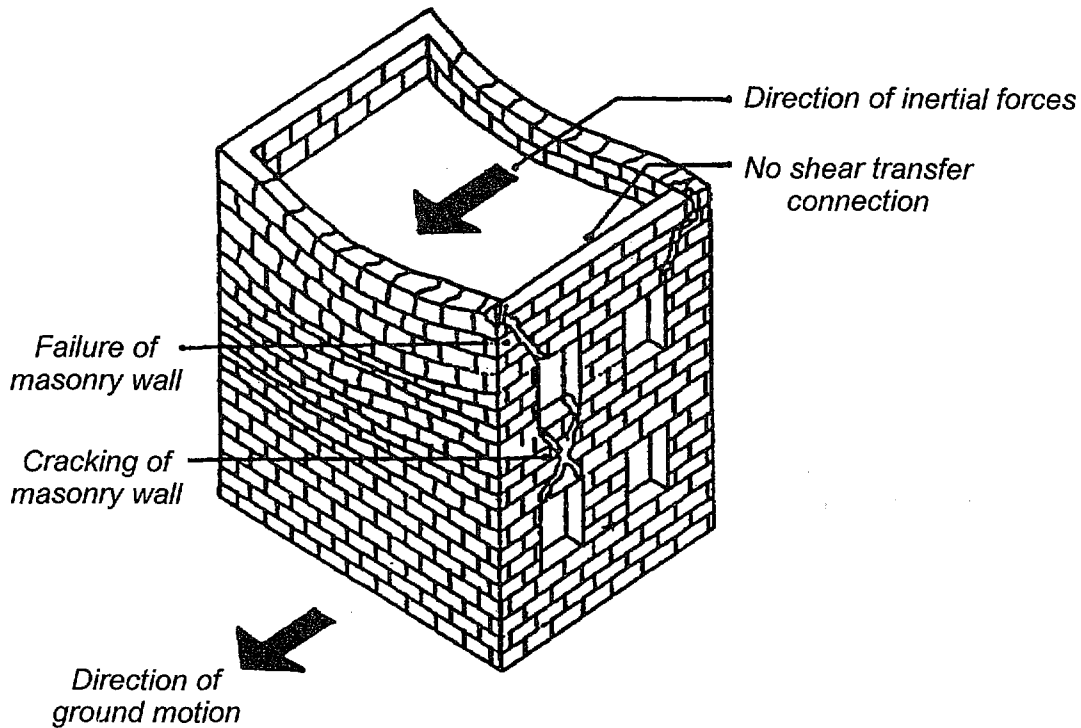


Diagram of Corner Failure

Figure 7-11 Diagram of Corner Damage (from City of Los Angeles, 1991)

The FEMA 273 equation for toe crushing is used. Post-crack displacement capacity is assumed to be negligible.

### 7.2.16 Out-of-Plane Flexural Response

Out-of-plane failures are common in URM buildings. Usually they occur due to the lack of adequate wall ties as discussed in Table 7-1. When floor and roof ties are adequate, the wall may fail due to out-of-plane bending between floor levels. One mode of failure observed in experiments is rigid-body out-of-plane rocking occurring on three cracks: one at the top of the wall, one at the bottom, and one at midheight. The ultimate limit

state is that the walls rock too far and overturn. Important variables identified by ABK (1984) and Adham (1985) were the vertical stress on the wall, the height-to-thickness ratio of the wall, and the input velocity provided to the wall by the diaphragms. As rocking increases, the mortar and masonry units at the crack locations can degrade, and residual offsets can occur at the crack planes.

ABK (1984) and Adham (1985) provide a graph, based on ABK (1981c), showing the relationship between the velocity at the top and bottom of the piers, the overburden ratio of superimposed load over wall load,